Adsorption of Gaseous Ethylamine on H-Form Strong-Acid Ion Exchangers

Equilibrium isotherms and kinetic data for sorption of ethylamine on two different H-form ion exchangers (a homogeneous gel type and a biporous MR type) have been determined experimentally by the gravimetric method. The gaseous amine is adsorbed on the dry resins according to an acid-base neutralization reaction, and the saturation capacity coincides with the exchange capacity of the resin. For the gel-type resin, the equilibrium is less favorable and the isotherm is almost linear over the experimental range.

The kinetic data also reflect the structural difference between the two adsorbents. In the MR-type resin, the sorption rate is controlled by macropore diffusion with rapid equilibration of the adsorbed phase within the microparticles. Since the equilibrium isotherm is highly favorable, approaching the irreversible limit, the uptake curves are well represented by the 'shrinking core' model. Diffusion in the gel-type resin is much slower and the pore diffusivities are smaller by several orders of magnitude, presumably reflecting the smaller effective pore diameter.

These results suggest that the MR-type resin is a potentially useful adsorbent for removal of traces of light amines from industrial gases.

Hiroyuki Yoshida
Department of Chemical Engineering
University of Osaka Prefecture
Sakai 591, Japan

Douglas M. Ruthven
Department of Chemical Engineering
University of New Brunswick
Fredericton, N.B., Canada E3B 5A3

Introduction

Gaseous amines and ammonia are generated in various chemical processes including the manufacture of cellophane, rayon and paper, as well as in sewage disposal and in the food processing industries. Because of their strong smell, it is important to remove these compounds from the waste gases and this has been traditionally accomplished by water washing or combustion. More recently the possibility of an adsorption process has been considered, since this would have the potential advantage of allowing recovery of the amines in concentrated form. There have been some preliminary industrial studies on the possibility of using carbon adsorbents, in either granular or fiber form, in this application, but few data are available to allow a quantitative evaluation of such a process. As an alternative to the use of carbon adsorbents, we have investigated the possibility of using a dry H-form strong-acid ion-exchange resin, which has the advantage of a more favorable equilibrium relation and easier desorption. The first results of our studies, which are reported here, suggest that such a process is both technically and economically feasible.

Correspondence concerning this paper should be addressed to H. Yoshida.

In contact with a H-form ion exchanger, the gaseous amine species are immobilized on the resin by the acid-base neutralization reaction:

$$R \cdot H + R' - NH_2 \rightleftharpoons R \cdot NH_3 - R' \qquad (1)$$

where $R' - NH_2$ denotes the amine, and $R \cdot NH_3 - R'$ denotes the amine-resin complex. The amine may be recovered by elution with caustic soda:

$$R \cdot NH_3 - R' + NaOH \rightarrow R \cdot Na + R' - NH_2 + H_2O \qquad (2)$$

and the resin is finally regenerated by acid:

$$R \cdot Na + HX \rightleftharpoons R \cdot H + NaX \qquad (3)$$

Ion exchange coupled with chemical reaction has been studied by Helfferich (1965), Blickenstaff (1967), Warner and Kennedy (1970), Graham and Dranoff (1972), Dana and Weelock (1974), Native et al. (1975), Kataoka et al. (1977), Höll and Sontheimer (1977), Kataoka and Yoshida (1981), Schmuckler

(1984), Höll (1984), Streat (1984), Yoshida et al. (1986a, b), and Yoshida and Kataoka (1986, 1987). Yoshida and Kataoka (1986, 1987) have shown that amine species in aqueous solution are adsorbed strongly on H-form strong-acid ion exchangers according to Eq. 1. However, no results for adsorption of gaseous amine on a dry H-form resin have been presented.

In the present work, equilibrium isotherms and kinetic data for sorption of gaseous ethylamine on two different H-form strong-acid ion exchangers (a homogeneous gel-type and a biporous MR-type) have been determined experimentally by the gravimetric method. The effects of the bulk gas-phase pressure, particle diameter, and temperature on the adsorption rate are reported. Intraparticle effective diffusivities are calculated from the experimental uptake data in order to establish the intraparticle mass transfer mechanism, and the uptake data are discussed in relation to the 'shrinking core' model (Yagi and Kunii, 1953; Weisz and Goodwin, 1963). The present results obtained for the gaseous amine are compared with the earlier results for the adsorption of similar amine species from aqueous solution, and the similarities and the differences in behavior are discussed.

Experimental Studies

The experimental systems and conditions are shown in Table 1. Two different H-form ion-exchange resins were used in order to assess the possibility of developing an adsorption system for the removal and/or recovery of gaseous amines: a homogeneous gel-type (DIAION SK1B and a biporous macroreticular (MR) resin (Diaion HPK25). The resin particles were dried at 323 K in the atmosphere for two days, and average particle diameters were measured after dehydration by scanning electron microscopy. Particles of reduced size, obtained by crushing the original resin particles, were used to establish the effect of the particle size on the uptake data.

The exchange capacity of the 'dry resin' was determined by the batch method. A sample of the H-form resin was converted to Na-form by contacting with 0.1 mol/dm^3 caustic soda solution. The reaction is expressed by the following irreversible neutralization reaction:

$$R \cdot H + NaOH \rightarrow R \cdot Na + H_2O \qquad (4)$$

The residual concentration of caustic soda in the solution was analyzed by the neutralization titration method using a methylorange indicator. The exchange capacity Q' (mol/kg) was calculated according to the mass balance equation:

$$Q' = \frac{V}{W} \cdot \Delta c \qquad (5)$$

where V, W, and Δc are respectively the volume of the solution (m^3), the weight of the resin particles (kg), and the change in the concentration of caustic soda (mol/m^3).

Ethylamine was used as the test adsorbate in a gravimetric system consisting of a Cahn vacuum microbalance. The resin particles (about 16 mg) were dried at 323 K in the atmosphere for two days. The sample was then placed on the pan of the microbalance and dehydrated under vacuum ($P \sim 10^{-2}$ Pa) for one day at the experimental temperature.

Since the isotherm for the MR-type resin proved to be highly favorable, kinetic measurements (runs 4–14) were made by the integral method from an initial amine pressure close to zero to a final pressure which was varied from 17 to 8,000 Pa. Some additional differential measurements were made in the low-pressure region in order to establish the detailed form of the isotherm. Since the isotherm for the gel-type resin was much less favorable, measurements were made differentially (runs 15–19). Following the establishment of steady state, additional increments of the amine were added without prior evacuation.

Results and Discussion

Physical properties of ion exchangers

The physical properties of the resins are summarized in Table 2. A particle of MR-type resin HPK25 consists of uniform microspherical resin particles. The diameter of the microsphere (d_{ms}) and the void fraction of the macropores (ϵ_p) were mea-

Table 1. Experimental Systems and Conditions

Resin	Amine	Run No.	Particle Dia., mm	Pres. Pa	Pres. Change	Temp. K
Diaion HPK25 (MR-Type)	Ethylamine b. p. = 289.6 K M. W. = 45.08	1	0.499	1.23	Differentially (Nos. 1-3)	338
		2		3.49		
		3		13.3		
		4		17.5	Integral step (Nos. 4–14)	
		5		97.3		
		6		305	Initial Pressure 0.013 Pa	
		7		617		
		8		1,570		
		9		7,990		
		10	0.835	17.5		
		11	0.115 (Crushed)	16.1		
		12	0.260 (Crushed)	21.2		
		13	0.499	7,980		309
		14		7,990		323
Diaion Sk1b (Gel-Type)		15	0.0875 (Crushed)	3.57	Differentially (Nos. 15–19)	338
		16		10.1		
		17		54.8		
		18		139		
		19		336		

Table 2. Physical Properties of Ion Exchangers

	HPK25 (MR-Type)	SK1B (Gel-Type)
Degree of Crosslinking (wt. %)	25	8
Particle Density (g/cm³ Particle) (Dried at 1.3×10^{-2} Pa for 1 d)	0.949	1.24
Void fraction of macropore (ϵ_p)	0.33*	
Diameter of Microspherical Resin Particle (d_{ms}), nm	76.6**	
Exchange Capacities, mol/kg		
Dried at 323 K in Atmosphere for 2 d (Q')	3.715	3.847
After dehydration at 1.3×10^{-2} Pa for 1 d (Q)	4.762	4.840
Equilibrium Coefficients (338 K)		
Saturation Capacity of Ethylamine (q_s), mol/kg	4.83	
Equilibrium Constant of Langmuir Equation (b') [1/Pa] at 338 K	0.598	
Dimensionless Henry's Law Constant ($K = bq_s$) at 338 K	10^7	3,000

*Measured by porosimetry (Yoshida et al., 1985)
**Measured by a scanning electron microscope (Yoshida et al., 1985)

sured after dehydration. The distribution curve of macropore diameter showed a peak at 57 nm, as reported elsewhere (Yoshida et al., 1985). The exchange capacity (Q') after drying at 323 K in the atmosphere for two days is smaller than the exchange capacity (Q) of a resin sample dehydrated in the microbalance system at about 10^{-2} Pa for one day, because the weight of the resin particles decreases by about 22% during dehydration.

Equilibria

Figure 1 shows the experimental equilibrium isotherms at 338 K for ethylamine on the two H-form ion-exchange resins. It is evident that the equilibrium for the MR-type resin is very favorable, and under most practical conditions the isotherm may be considered as rectangular. Adsorption on the gel-type resin is not as strong, so that the isotherm is less favorable. In the case of MR-type resin, since Table 2 shows that the saturation capacity of the ethylamine (q_s') is close to the exchange capacity (Q) which was obtained after dehydration, it may be assumed that there is no physical adsorption. The reaction between the H-form resin (R · H) and the amine gas (R′ – NH_2) may

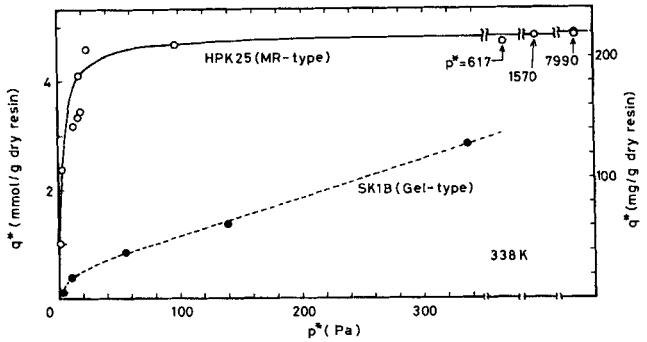

Figure 1. Equilibrium isotherms of ethylamine for MR-type and gel-type H-form resins.

therefore be expressed by Eq. 1, which is simply the neutralization reaction for acidic R · H and basic R′ – NH_2.

Such a mechanism is formally equivalent to chemisorption at the hydrogen ion sites; one may therefore expect that since such sites are reasonably well separated, the equilibrium isotherm should approximate to the Langmuir model:

$$\frac{q^*}{q_s} = \frac{b'p}{1 + b'p} = \frac{bC}{1 + bC} \tag{6}$$

The equilibrium data for the MR-type resin do indeed conform to this equation, and the relevant parameters are given in Table 2. It is evident from Figure 1 that the isotherm is highly favorable and, over the relevant pressure range, is in fact close to the rectangular limit. Adsorption on the gel-type resin is much weaker and the isotherm deviates only slightly from linearity.

Yoshida and Kataoka (1986, 1987) have investigated the adsorption of several amines [C_0(ammonia)—C_{12}(Laurylamine)] from aqueous solution onto the same H-form resins. The equilibrium data showed that the amines were strongly adsorbed on both resins. The isotherms for the amines of C_0—C_4 were represented by a corrected Langmuir expression. The saturation capacities for both resins were close to their exchange capacities, and the values derived for the adsorption equilibrium constants for both resins were very similar. The behavior of the MR-type resin is thus seen to be similar in vapor and liquid phases, whereas the gel-type resin behaves differently, exhibiting a much lower affinity in the vapor phase.

A possible explanation for this difference is as follows. The resin particles swell in aqueous solution and shrink in the gaseous system due to dehydration. Since the degrees of crosslinking of the gel-type resin and the MR-type resin are 8 and 25%, respectively, the degree of shrinkage caused by dehydration of the gel-type resin will be higher than that for the MR-type resin. As a result of this shrinkage, in the gel-type resin a relatively large fraction of H^+ ions may be covered by the resin matrix and thus prevented from close contact with the amine molecules, thus reducing the energy of interaction between the amine and H^+ ion. The MR-type resin also shrinks, but since the degree of crosslinking is three times as high as that of the gel-type resin, all pores around the fixed H^+ ions may well remain open so that the amine molecules can still reach all the fixed H^+ sites. Such a hypothesis is obviously speculative, but it can explain why the equilibrium isotherm for the MR-type resin in the gaseous system is very favorable and is similar to that for the aqueous system, while for the gel-type resin, the isotherm for the gaseous amine is much less favorable.

Modeling of uptake curves

Figures 2–4 show the experimental uptake data for the MR-type resin, plotted as fractional approach to equilibrium (F) vs. time. It is evident from Figure 2 that the rate of adsorption increases strongly with increasing pressure, and it may be seen from Figure 3 that the half time is approximately proportional to the square of the particle diameter, suggesting that the sorption rate is controlled by macropore diffusion and the diffusion within the microparticle must be very rapid. The possibility of external fluid-side resistance can be excluded, since the gas phase is pure ethylamine vapor. This conclusion is supported by the initial rate data which show that, in the initial region, the uptake increases approximately linearly with the square root of

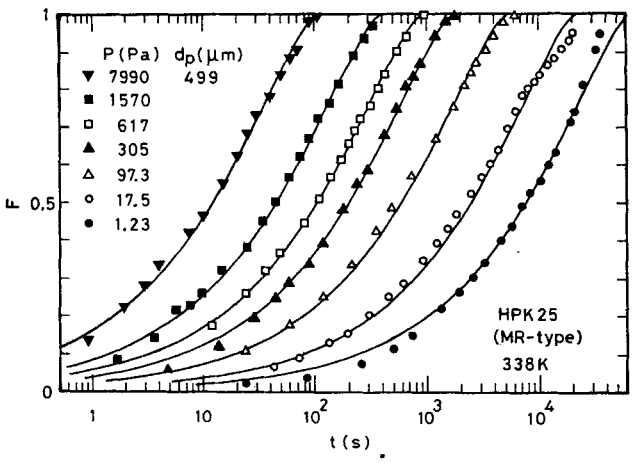

Figure 2. Experimental uptake curves obtained in integral measurements showing the effect of pressure on uptake rate for ethylamine on MR-type (H-form) resin.

●, Run 1; ○, Run 4; △, Run 5; ▲, Run 6; □, Run 7; ■, Run 8; ▼, Run 9. Lines are calculated from Eq. 17 with parameters given in Tables 2 and 4.

time. The uptake rate also increases with temperature (Figure 4), but since the measurements were made only over limited temperature range, the difference between the two curves is relatively small.

The sorption process may therefore be modeled as Fickian diffusion within the macropores of the gross particle with rapid equilibration between the intraparticle fluid phase and the adsorbed phase within the microparticles. For such a system, the differential mass balance equation, assuming a constant pore diffusivity, is:

$$(1-\epsilon_p)\frac{\partial q}{\partial t}+\epsilon_p\frac{\partial C}{\partial t}=\epsilon_p D_p\frac{1}{r^2}\frac{\partial}{\partial r}\left(r^2\frac{\partial C}{\partial r}\right) \tag{7}$$

where $q(r, t)$ and $C(r, t)$ denote the local concentrations in the adsorbed and fluid phase, respectively. The appropriate initial

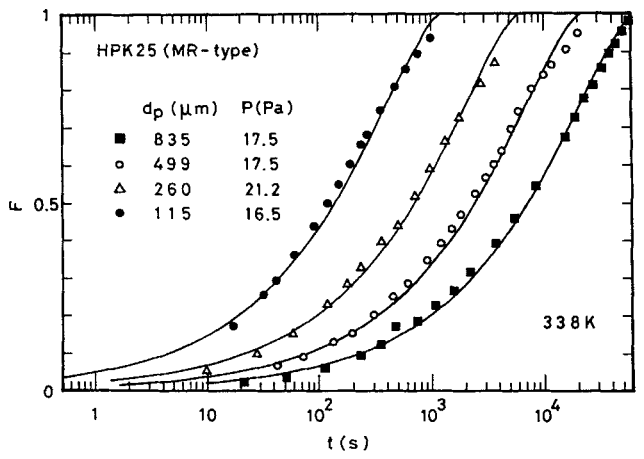

Figure 3. Experimental (integral) uptake curves for MR-type (H-form) resin showing effect of particle size.

○, Run 4; ■, Run 10; ●, Run 11; △, Run 12. Lines are calculated from Eq. 17 with parameters given in Tables 2 and 4.

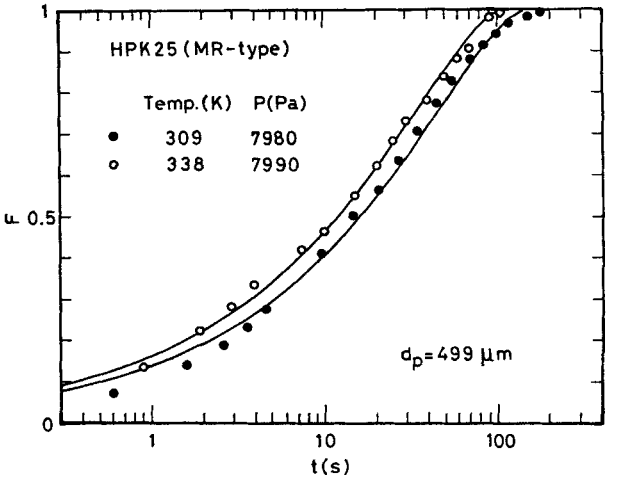

Figure 4. Experimental (integral) uptake curves for MR-type (H-form) resin showing effect of temperature.

○, Run 9; ●, Run 13. Lines are calculated from Eq. 17 with parameters given in Tables 2 and 4.

and boundary conditions are:

$$q(r,0)=q_i;\quad q(r_o,t)=q_o;\quad \left.\frac{\partial C}{\partial r}\right|_{r=0}=0$$
$$C(r,0)=C_i;\quad C(r_o,t)=C_o; \tag{8}$$

If the equilibrium relationship is linear ($q = KC$), Eq. 7 may be written as:

$$\frac{\partial C}{\partial t}=\frac{\epsilon_p D_p}{\epsilon_p+(1-\epsilon_p)K}\cdot\frac{1}{r^2}\frac{\partial}{\partial r}\left(r^2\frac{\partial C}{\partial r}\right) \tag{9}$$

which is formally identical to the standard form of the diffusion equation with an effective diffusivity given by:

$$D_{\text{eff}}=\frac{\epsilon_p D_p}{\epsilon_p+(1-\epsilon_p)K} \tag{10}$$

The solution has been given by Crank (1975):

$$F=\frac{\bar{q}-q_i}{q_o-q_i}=6\left(\frac{D_{\text{eff}}t}{r_o^2}\right)^{1/2}\cdot\left\{\sqrt{\pi}+2\sum_{n=1}^{\infty}\text{ierfc}\frac{nr_o}{\sqrt{D_{\text{eff}}t}}\right\}-3\left(\frac{D_{\text{eff}}t}{r_o^2}\right) \tag{11}$$

When the equilibrium follows a Langmuir expression (Eq. 6),

$$\frac{dq}{dC}=\frac{bq_s}{(1+bC)^2}=bq_s(1-q/q_s) \tag{12}$$

so, neglecting the accumulation within the macropores in comparison with the accumulation in the adsorbed phase, which is an excellent approximation for adsorption from the gas phase, we have in place of Eq. 9:

$$\frac{\partial q}{\partial t}=\frac{\epsilon_p D_p}{(1-\epsilon_p)bq_s}\cdot\frac{1}{r^2}\cdot\frac{\partial}{\partial r}\left\{\frac{r^2}{(1-q/q_s)^2}\cdot\frac{\partial q}{\partial r}\right\} \tag{13}$$

which is equivalent to the Fickian diffusion equation with a concentration-dependent effective diffusivity given by:

$$D = \frac{\epsilon_p D_p}{(1 - \epsilon_p) b q_s (1 - q/q_s)^2} \tag{14}$$

Since Eq. 13 is nonlinear, an analytic solution cannot be obtained but a numerical solution for the relevant initial and boundary conditions has been given by Garg and Ruthven (1972). The dimensionless uptake curve (F vs. $D_o t/r_o^2$) is a function of the concentration step, measured by the parameter $\lambda = q_o/q_s$, over which the curve is measured but the actual form of the curve differs only slightly from that for a linear system (Eq. 11). In particular the initial uptake is still approximately linear in $\sqrt{t}$.

When the concentration approaches the saturation limit, an alternative approach based on the approximation of a rectangular equilibrium isotherm is preferable. The concentration profile within the particle assumes the well-known 'shrinking core' form, illustrated in Figure 5. The solution for the uptake curve under the conditions was obtained by Yagi and Kunii (1953) and has since been applied in several different contexts—see, for example, Weisz and Goodwin (1963), Levenspiel (1966), Wen (1968). The resin particle is divided into a central core of unreacted R · H and an outer shell of R · NH_3 – R′. Since the isotherm is rectangular, at the concentration front in the macropore ($r = \delta$) the amine molecules are completely adsorbed on the H^+ ion sites according to the reaction of Eq. 1. The adsorbed-phase concentration of the amine (q) is therefore uniform throughout the shell $\delta \leqq r \leqq r_o$ and equal to q_o which is essentially equal to q_s when the isotherm is completely rectangular. Under these conditions the pseudosteady-state approximation applies and Eq. 7 reduces to:

$$\frac{\partial}{\partial r}\left(r^2 \frac{\partial C}{\partial r}\right) = 0, \qquad (\delta \leqq r \leqq r_o) \tag{15}$$

with the initial and boundary conditions:

$$\delta|_{t=0} = r_o;\ C|_{r=r_o} = 0;\ C|_{r=\delta} = 0;$$
$$\text{At } r = \delta\text{: } \epsilon_p D_p \left.\frac{dC}{\partial r}\right|_{r=\delta} = -\rho q_o \frac{d\delta}{dt} \tag{16}$$

The solution is:

$$\frac{6\,\epsilon_p D_p C_o}{\rho\, q_o r_o^2} t = 1 + 2(1 - F) - 3(1 - F)^{2/3} \tag{17}$$

which provides a simple implicit expression for the dimensionless uptake curve.

When the concentration step in an integral experiment approaches the saturation limit ($\lambda > 0.8$), the form of the concentration profile and the corresponding uptake curve approach the irreversible model (Eq. 17). This is illustrated in Table 3 which shows, for the same concentration ratio (q_o/C_o), a comparison between the half times calculated from the Langmuir and irreversible models.

Analysis of experimental uptake curves

The equilibrium isotherm for the gel-type resin is approximately linear over the experimental range, and the uptake curves for this adsorbent were therefore matched to Eq. 11 to determine the effective diffusivity values. Using the equilibrium data, the pore diffusivity values could then be found from Eq. 10. The values of D_{eff} and D_p so derived are summarized in Table 4.

The uptake curves for the MR-type resin were almost all measured under integral conditions such that q_o is close to the saturation limit (see Table 4), and these curves were therefore analyzed according to the irreversible model (Eq. 17). The parameters so derived are given in Table 4 and the fits of the experimental and theoretical curves are shown in Figures 2–4.

Figure 6 shows that the pore diffusivities derived from measurements with different particle sizes are constant, thus providing evidence that the model used to interpret the kinetic data is essentially correct. Although the apparent diffusivities, derived by matching the uptake curves directly to Eq. 11, show a monotonic increase with concentration, the pore diffusivities (derived from Eq. 17) are essentially constant at the lower pressures,

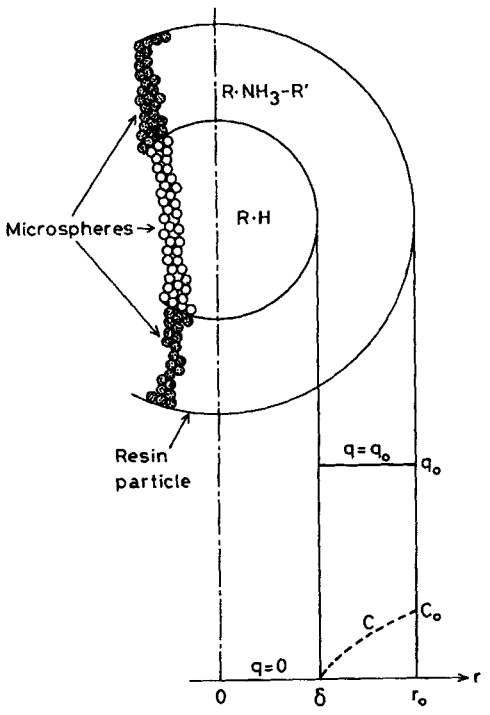

Figure 5. Concentration distribution in a MR-type resin particle.

Table 3. Comparison between Langmuir and Irreversible Models for Macropore Diffusion Control

		Half Time – Eq. 17
$\lambda = q_o/q_s$	$f = D_{\text{eff}}/D_o$	Half Time – Langmuir Model
0.5	2.8	0.85
0.6	3.6	0.88
0.7	5.0	0.92
0.8	7.2	0.95
0.9	16.5	0.99
0.95	33	1.0

Table 4. Diffusivity Data for Ethylamine in MR-Type and Gel-Type Resins (Vapor Phase)

Run No.	Pres. Step Pa	T K	$D_{eff} \times 10^{13}$ $m^2 \cdot s^{-1}$	$\epsilon_p D_p \times 10^9$ $m^2 \cdot s^{-1}$	$\lambda = q_o/q_s$
HPK25 (MR-Type, $K = 10^7$)					
4	0–17.5	338	8.4	200	0.975
5	0–97.3	338	29.2	195	0.936
6	0–305	338	102	174	0.902
7	0–617	338	152	187	0.998
8	0–1570	338	537	175	1.0
9	0–7990	338	2,130	130	1.0
10	0–17.5	338	8.7	191	0.864
11	0–16.1	338	8.5	194	0.975
12	0–21.2	338	8.5	187	0.975
13	0–7980	309	1,390	97	
14	0–7990	323	1,780	109	
SK1B (Gel-Type, $K = 3{,}000$)					
16	0–10.1	338	0.253	0.076	
17	10.1–54.8	338	0.223	0.067	
18	54.8–139	338	0.214	0.064	
19	139–336	338	0.122	0.037	

decreasing somewhat at the higher pressures (Figure 7). This satisfies the assumption of a constant diffusivity which is implicit in the derivation of Eq. 17. A similar trend is observed in the pore diffusivities for the gel-type resin although the order of magnitude is much smaller. Such behavior is typical of a macropore diffusion system in which Knudsen diffusion is dominant at low pressures with an increasing contribution from molecular diffusion at higher pressures. The modest temperature dependency of the pore diffusivity (runs 9, 13, and 14) is also consistent with this interpretation. However, the very large difference in pore diffusivity between the gel- and MR-type resins cannot be explained in that way and suggests that there must be significant steric hindrance in the small pores of the gel-type resin.

Also included in Table 4 are the effective diffusivities for the MR-type resin derived by matching the uptake curves to the linear model (Eq. 11). It is clear that the effective diffusivities increase directly with the magnitude of the pressure step. However, the above analysis shows that this is in fact due to the nonlineality of the equilibrium relationship; the pore diffusivity is almost independent of pressure.

Yoshida and Kataoka (1987) also investigated adsorption of several light amines from aqueous solution into the same H-form resins. The kinetic data were analyzed in terms of the irreversible model, including external film and intraparticle diffusion (homogeneous model) resistances. The intraparticle effective diffusivities for monoethanolamine and diethylamine were found to be two to five times larger in the gel-type resin as compared with the MR-type resin. This result stands in marked contrast to the present data for vapor-phase adsorption of ethylamine, which show the effective diffusivities in the gel-type resin to be substantially smaller than those in the MR-type resin. Furthermore, the effective diffusivity values for the aqueous system (order 10^{-10}–$10^{-11} m^2 \cdot s^{-1}$ in the gel-type resin) are much higher than those for the vapor-phase system. These differences can be largely accounted for by the difference in adsorption equilibrium. The effective diffusivity in the homogeneous model (D_{eff}) is related to the pore diffusivity (D_p) by:

$$D_{eff} \approx 1.65 \frac{\epsilon_p D_p C_o}{q_o} \tag{18}$$

as derived in the Appendix. The concentration ratio (q_o/C_o) is in the range 15–300.

Table 5 shows the effective pore diffusivities for monoethanolamine and diethylamine (liquid phase), as calculated from the data of Yoshida and Kataoka (1987) according to Eq. 18. The effective pore diffusivity for the gel-type resin ($\epsilon_p D_p$) are about a hundred times larger in the liquid than that in the vapor

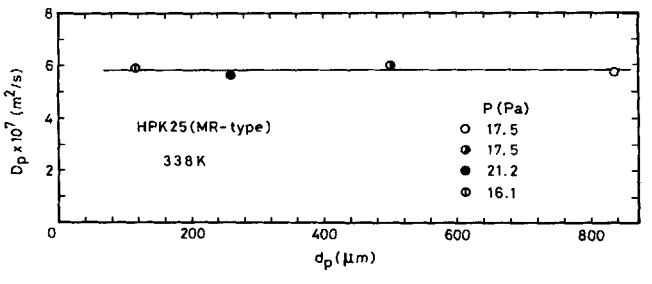

Figure 6. Effect of particle diameter on pore diffusivity of ethylamine for MR-type (H-form) resin.

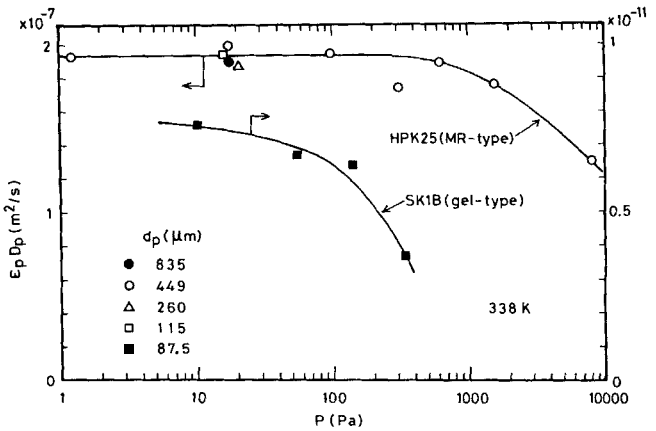

Figure 7. Effect of bulk pressure on pore diffusivity of ethylamine for MR-type and gel-type H-form resins.

Table 5. Pore Diffusivity of Monoethanolamine and Diethylamine in MR-Type and Gel-Type Resins for Liquid-Phase Systems

	$\epsilon_p D_p \times 10^9$, $m^2 \cdot s^{-1}$	
C_o mol/dm^3	Monoethanolamine	Diethylamine
HPK25 (MR-Type)		
0.01	7.47	3.68
0.5	2.31	1.83
0.1	1.76	1.23
0.25	0.721	
0.51	0.434	
SK1B (Gel-Type)		
0.01	14.5	15.8
0.053	10.8	10.4
0.1	8.30	9.64
0.25	4.39	4.19
0.51	2.57	

system, although the molecular diffusivity in the liquid phase is of course much smaller than that in the vapor phase. This may reflect swelling of the resin which would reduce steric hindrance in the aqueous system.

On the other hand, the effective liquid-phase pore diffusivities for the MR-type resin are of the same order as for the gel-type resin and about 100 times smaller than for the vapor-phase system. This may suggest that, while diffusion of the light amine vapors in the MR-type resin is controlled mainly by macropore resistance, in the aqueous system micropore resistance is probably more significant.

Notation

b = equilibrium constant of Langmuir equation (Eq. 6), m^3/mol
b' = equilibrium constant of Langmuir equation (Eq. 6), $1/Pa$
C = concentration in macropore, mol/m^3
C_o = bulk gas phase concentration, mol/m^3
Δc = change in liquid-phase concentration of caustic soda, mol/m^3
D_{eff} = intraparticle effective diffusivity, m^2/s
D_p = macropore diffusivity for MR-type resin and micropore diffusivity for gel-type resin, m^2/s
D_o = limiting diffusivity at low concentration (for Eq. 14 with $q \rightarrow 0$), m^2/s
d_{ms} = diameter of microspherical resin particle of MR-type ion exchanger, nm
F = fractional attainment of equilibrium
f = D_{eff}/D_o
K = Henry's Law constant = bq_s, dimensionless
P = pressure in bulk gas phase, Pa
Q = exchange capacity of resin which was dehydrated at 1.3×10^{-2} Pa for 1 day, mol/kg
Q' = exchange capacity of resin which was dried at 323 K in atmosphere for 2 days, mol/kg
q = adsorbed-phase concentration, mol/kg
$\overline{q}'$, $\overline{q}$ = mean adsorbed-phase concentration, mol/kg, mol/m^3
q'^*, q^* = adsorbed-phase concentration in equilibrium with p, mol/kg, mol/m^3
q'_i, q_i = initial adsorbed-phase concentration, mol/kg, mol/m^3
q'_o, q_o = adsorbed-phase concentration in equilibrium with C_o, mol/kg, mol/m^3
q'_s, q_s = saturation capacity, mol/kg, mol/m^3
r = radial dimension of resin particle, m
r_o = radius of resin particle, m
t = time, s
V = volume of caustic soda solution, m^3
W = weight of resin particles, kg

Greek letters

δ = distance from the center of resin particle to reaction plane, m
ϵ_p = void fraction of macropore
ρ = density of resin particle, kg/m^3
$\lambda = q_o/q_s$

Literature Cited

Blickenstaff, R. A., J. W. Wargner, and J. S. Dranoff, "The Kinetics of Ion Exchange Accompanied by Irreversible Reaction: I. Film Diffusion Controlled Neutralization of A Strong Acid," *J. Phys. Chem.*, **71**, 1665 (1967).

Crank, J., *The Mathematics of Diffusion*, Clarendon Press, Oxford, 2nd ed., 91 (1975).

Dana, P. R., and T. D. Weelock, "Kinetics of Moving Boundary Ion Exchange Process," *Ind. Eng. Chem. Fund.*, **13**, 20 (1974).

Garg, D. R., and D. M. Ruthven, "The Effect of the Concentration Dependence of Diffusivity on Zeolitic Sorption Curves," *Chem. Eng. Sci.*, **27**, 417 (1972).

Graham, E. E., and J. S. Dranoff, "Kinetics of Anion Exchange Accompanied by First Irreversible Reaction," *AIChE J.*, **18**, 608 (1972).

Helfferich, F., "Ion Exchange Kinetics: V. Ion Exchange Accompanied by Reaction," *J. Phys. Chem.*, **69**, 1178 (1965).

Höll, W., "Optical Verification of Ion Exchange Mechanism in Weak Electrolyte Resin," *Reactive Polym.*, **2**, 93 (1984).

Höll, W., and H. Sontheimer, "Ion Exchange Kinetics of Protonation of Weak Acid Ion Exchange Resins," *Chem. Eng. Sci.*, **32**, 755 (1977).

Kataoka, T., and H. Yoshida, "Intraparticle Mass Transfer in Weak Acid Ion-Exchanger," *Can. J. Chem. Eng.*, **59**, 475 (1981).

Kataoka, T., H. Yoshida, and Y. Ozasa, "Intraparticle Ion Exchange Mass Transfer Accompanied by Irreversible Reaction," *Chem. Eng. Sci.*, **32**, 1237 (1977).

Native, M., S. Goldstein, and G. Schmuckler, "Kinetics of Ion Exchange Process Accompanied by Chemical Reactions," *J. Inorg. Nucl. Chem.*, **37**, 1951 (1975).

Levenspiel, O., *Chemical Reaction Engineering*, Wiley, New York, 346 (1966).

Sherwood, T. K., R. L. Pigford, and C. R. Wilke, *Mass Transfer*, McGraw-Hill, 18 (1975).

Schmuckler, G., "Kinetics of Moving-Boundary Ion-Exchange Processes," *Reactive Polym.*, **2**, 103 (1984).

Streat, M., "Kinetics of Slow Diffusing Species in Ion Exchangers," *Reactive Polym.*, **2**, 79 (1984).

Warner, R. E., and A. M. Kennedy, "Kinetics of Neutralization of Weak Electrolyte Ion Exchange Resins," *Macromol. Chem.*, **A4**, 1125 (1970).

Weisz, P. B., and R. D. Goodwin, "Combustion of Carbonaceous Deposits within Porous Catalyst Particles: I. Diffusion Controlled Kinetics," *J. Cat.*, **2**, 397 (1963).

Wen, C. Y., "Noncatalytic Heterogeneous Solid-Fluid Reaction Models," *Ind. Eng. Chem.*, **60**, 34 (1968).

Yoshida, H., and T. Kataoka, "Adsorption of Amines and Ammonia on H^+-Form Ion Exchanger," *Chem. Eng. Sci.*, **42**, 1805 (1987).

Yagi, S., and D. Kunii, "Theory on roasting of sulfide ore with uniform particle diameter in fluidized bed," *Kogyou-Kagaku-Zassi*, Japan, **56**, 131 (1953).

Yoshida, H., and T. Kataoka, "Recovery of Amine and Ammonia by Ion Exchange Method: Comparison of Ligand Sorption and Ion Exchange Accompanied by Neutralization Reaction," *Solvent Extraction and Ion Exchange*, **4**, 1171 (1986).

Yoshida, H., T. Kataoka, and S. Fujikawa, "Kinetics in a Chelate Ion Exchanger: I. Theoretical Analysis," *Chem. Eng. Sci.*, **41**, 2517 (1986a).

———, "Kinetics in A Chelate Ion Exchanger: II. Experimental," *Chem. Eng. Sci.*, **41**, 2525 (1986b).

Appendix

Consider a set of uniform spherical particles subject at $t = 0$ to a step change in sorbate concentration at the external surface. In the homogeneous diffusion model, regardless of the form of the equilibrium isotherm the uptake curve is given by Eq. 11 from which the half time ($t_{1/2}$) is found to be:

$$\frac{D_{eff} t_{1/2}}{r_o^2} = 0.03 \tag{A1}$$

On the other hand, if we consider a pore-diffusion-controlled system with irreversible adsorption, the uptake curve follows Eq. 17 and the half-time is given by:

$$\frac{6\,\epsilon_p D_p C_o}{r_o^2 q_o}\, t_{1/2} = 0.11 \tag{A2}$$

Despite the difference in the algebraic forms, the shapes of the curves represented by Eqs. 11 and 17 are similar, and the relationship between the diffusion parameters is

$$D_{eff} \doteq 1.65\, \epsilon_p D_p \frac{C_o}{q_o} \tag{A3}$$

Manuscript received Dec. 22, 1988, and revision received July 6, 1989.